



Nguyen, D. H., Lowenberg, M. H., & Neild, S. A. (2020). Frequency-Domain Bifurcation Analysis of a Nonlinear Flight Dynamics Model. *Journal of Guidance, Control, and Dynamics*.
<https://doi.org/10.2514/1.G005197>

Peer reviewed version

Link to published version (if available):
[10.2514/1.G005197](https://doi.org/10.2514/1.G005197)

[Link to publication record in Explore Bristol Research](#)
PDF-document

This is the author accepted manuscript (AAM). The final published version (version of record) is available online via American Institute of Aeronautics and Astronautics at <https://doi.org/10.2514/1.G005197>. Please refer to any applicable terms of use of the publisher.

University of Bristol - Explore Bristol Research

General rights

This document is made available in accordance with publisher policies. Please cite only the published version using the reference above. Full terms of use are available:
<http://www.bristol.ac.uk/red/research-policy/pure/user-guides/ebr-terms/>

Frequency-Domain Bifurcation Analysis of a Nonlinear Flight Dynamics Model

Duc H. Nguyen¹, Mark H. Lowenberg², and Simon A. Neild³
Department of Aerospace Engineering, University of Bristol, Bristol, BS8 1TR

This paper presents a methodology for systematically studying the nonlinear frequency responses of an aircraft model using numerical continuation with periodic forcing, thereby presenting an extension of conventional bifurcation analysis in flight dynamics applications. The motivation is to identify nonlinear phenomena in the frequency domain that are absent in linearized models - upon which many control law designs are based - and which therefore risks degrading the performance or robustness of the linear-model based controllers. Since the aerospace industry typically uses linearizations in controller design, both open and closed-loop behaviors are considered. When the example aircraft considered here is forced with small control surface deflections, highly nonlinear responses are observed. This includes period-doubling bifurcations, fold bifurcations leading to existence of multiple solutions, quasi-periodic motions, and formation of isolas. Closed-loop responses of a proportional stability augmentation controller for this aircraft become out of phase with the linear prediction at low forcing frequencies when the aircraft operates at high angle of attack. To address these behaviors, the methodology is extended by employing two-parameter continuation of the controller gain to assess its effectiveness in those nonlinear regions, where linear controller design techniques cannot be used. Time histories are used to verify the results.

Nomenclature

A	=	elevator forcing amplitude (deg)
q	=	pitch rate (deg/s)

Presented as Paper 6.2020-0605 at the AIAA SciTech 2020 Forum, Orlando, FL, 6-10 January.

¹ PhD student, Department of Aerospace Engineering, Student Member AIAA.

² Professor of Flight Dynamics, Department of Aerospace Engineering, Senior Member AIAA.

³ Professor of Nonlinear Structural Dynamics, Department of Aerospace Engineering.

t	=	time (s)
V	=	total velocity (m/s)
α	=	angle of attack (deg)
δ_e	=	elevator (deg)
Δ	=	incremental, relative to trim value (used as prefix)
θ	=	pitch angle (deg)
γ	=	flight path angle (deg)
ω	=	elevator forcing frequency (Hz)

I. Introduction

Aircraft controllers are typically designed using linear techniques at a number of operating points across the flight envelope. The resulting controllers are then combined into a single nonlinear gain-scheduled controller. Although the linear design techniques offer many advantages, most importantly the availability of closed-form solutions, this approach may be questionable when the aircraft operates in highly nonlinear regions. Under such conditions, it is likely that the intended loop-shaping objectives will not be met - and the controller effectiveness may become severely degraded in cases where strong nonlinearities such as multiple solutions and hysteresis arise. These problems can occur during extreme maneuvering for a fighter aircraft, or in upsets and loss-of-control situations for a civilian aircraft. Therefore, it is important to determine the extent to which the linear model can capture the dynamics before the predicted response no longer adequately matches the actual response of the full nonlinear model. This paper proposes a novel approach to study this problem by using numerical tools from bifurcation analysis to characterize the nonlinear behavior of the system coupled with a harmonic oscillator. This permits the assessment of frequency-domain-based assumptions used in linear control design, such as stability margins or superposition. The objective is to identify regions in which linear-model based design is questionable.

Nonlinear phenomena in flight dynamics have been widely documented, and much research has been done to combine nonlinear analysis with classical flight dynamics and control theory to improve performance and safety. Since their first application on an aircraft model [1], bifurcation analysis and continuation methods have gained recognition in the flight dynamics research community as a powerful tool in studying nonlinear phenomena at high angle of attack

commonly found for high-performance fighter jets [2-7]. More recently, the tool has been used on civil applications to study airliner upsets and loss-of-control [8-10] following accidents such as Air France flight 447. Specifically, it is shown in [9] that dangerous upset conditions like entry into oscillatory spins caused by an incorrect pilot response from a spiral dive can be characterized as stable attractors in the phase space. A linear representation of the aircraft cannot capture this behavior and as a result, a controller based on this linearization may be unable to recover the aircraft from upsets outside the normal operating envelopes. Indeed, in [10], the analysis was repeated on the same aircraft model coupled with a linear gain-scheduled controller and was successful in identifying upset attractors that are still beyond the controller's capability. Analysis on the effect of controller gains in eliminating those regions of upsets was also carried out in [10], which proved useful in comparing the robustness of different controller designs.

While most published work on flight dynamics and control using continuation methods focus on studying equilibrium solutions to satisfy handling quality requirements in the time domain, very little has been done to study periodic solutions of a forced system to satisfy frequency-domain criteria. In linear system theory, a harmonic input produces a harmonic output of the same frequency whereas the output of a nonlinear system may contain multiple frequencies. Moreover, a smooth variation in forcing frequency or amplitude in a linear system produces smooth changes in response amplitude and phase. In a nonlinear system, the response is dependent on both forcing frequency and amplitude and may give rise to bistable solutions. A smooth variation in input frequency could then, for example, cause abrupt changes in both amplitude and phase, known as jump phenomena. Forced oscillation of nonlinear systems has been studied in depth, such as in [11, 12], but its application has so far been limited to primarily structural engineering [13-16].

Despite limited studies in the flight dynamics context, the problem of nonlinear oscillation can arise in aircraft with complex and highly augmented flight control systems due to coupling between the aircraft's natural modes, structural modes, aerodynamics, and the control system itself. During a series of low altitude and high speed test flights outside the operational envelope, a B-2 encountered residual pitch oscillations in response to a doublet input on control surfaces [17]. The phenomenon was not predicted by analytical methods, wind tunnel tests or previous flutter tests, and subsequent work determined the possible cause to be a complex interaction between transonic aerodynamics and aeroelasticity. The study concluded that a pilot should stay clear of that region in the envelope and made no mention of the B-2's complex and highly classified stability augmentation system, which cannot be disabled in flight [17]. It is possible that the interaction between aerodynamic and structural dynamics had created a highly

nonlinear forced oscillation situation, which coupled with the flight control system and led to the pitch oscillation in question. This is demonstrated in [18], which showed that a controller designed for a rigid aircraft model has degraded performance when used on the non-rigid model of the same aircraft due to the reduced frequency separation between the rigid-body and flexible modes. Nevertheless, these studies still focus on the structural aspects of the aircraft, and there remains a gap in the literature around the topic of nonlinear interactions between the flight control system and the aircraft natural modes. The nonlinear phenomena mentioned above may cause violations of the frequency response design criteria, degrade the controller's performance and therefore compromise performance and safety, especially at high angle-of-attack and in regions outside the normal operational envelope.

Among the few studies on flight dynamics involving forced response using continuation methods are [19, 20]. In [19], a harmonic oscillator was coupled to an F/A-18 model with pilot (modeled as a simple proportional gain) in the loop: the objective was to predict pilot-induced oscillations through observation of rapid increases in output oscillation amplitudes as pilot gain parameter is varied. In [20], the harmonic oscillator was appended to the thrust vector deflection of an F-18 HARV model flying at very high angles of attack, where conventional control surfaces are ineffective. Although the ranges of forcing amplitude and frequency are relatively narrow (no more than 2° in amplitude and between 0.1 and 1 rad/s in frequency), the aircraft's response is extremely complex. Different combinations of the forcing parameters can result in period-1, period-2, period-4 or chaotic motions caused by a number of period-doubling and torus bifurcations. The study also identified cases in which the same input can result in period-1, period-2 or chaotic motions, suggesting a dependence on the initial conditions. This is caused by the coexistence of several stable attractors at the same frequencies, some of which are chaotic and, therefore, give rise to the aircraft's complex behavior. Since a linearization of the model is incapable of capturing these phenomena, knowledge of them is essential to designing an adequate controller.

This paper expands on the technique presented in [19, 20] to study an aircraft's forced responses, specifically by generating a nonlinear frequency response plot to assess the dynamics in the frequency domain. This method is applicable to both the open and closed-loop dynamics, which can be used to inform the control designer of the controller's validity by comparing its linear and nonlinear frequency responses, thereby determining regions in which the linearized and the full nonlinear model may behave differently. This technique also provides the possibility of capturing the effects of any unsteady (time-dependent) features in the model - which the evaluation of steady states in an autonomous (unforced) implementation would miss.

II. Methodology: Bifurcation Analysis of Periodically Forced Systems

Bifurcation analysis facilitates a systematic study of changes in qualitative behavior of a nonlinear dynamical system. This includes (but is not limited to) the existence of multiple solutions, jump phenomena and stability loss, which are clearly important in flight dynamics. One of the goals of bifurcation analysis is to produce a map of how the system's steady states change with respect to a control parameter (i.e. to construct a bifurcation diagram), and to provide information on the nature and stability of those solutions. This process requires solving the full nonlinear equations of motion of the system (such as an aircraft model), which can be very complex analytically. In practice, the equations are solved using numerical continuation, which utilizes a path-following algorithm to trace out the solutions of the system from an initial solution supplied by the user [21]. The varying control parameter in numerical continuation is called the continuation parameter. In a flight dynamics model, this can be elevator deflection, center of gravity position, or controller gain, for example. Bifurcation diagrams do not provide any information on the transient responses, such as how quickly the system converges to a steady state, so numerical simulations must always be performed to verify the results and understand the transient dynamics. More background on bifurcation analysis and continuation methods for autonomous (unforced) systems can be found in [2, 21]. In this paper, bifurcation analysis and continuation methods were implemented in the MATLAB environment using the Dynamical Systems Toolbox [22], which is a MATLAB implementation of the software AUTO [23].

Since the focus of this paper is on bifurcation analysis of a periodically forced system, we first explored the concept by applying the technique to a simple nonlinear system: the Duffing equation. This is a well-studied example (see [11, 12]) that describes a nonlinear mass-spring-damper system and is commonly used to demonstrate the common phenomena encountered in a nonlinear forced system. This spring generates a restoring force that is a summation of a term proportional to the linear displacement x and another term proportional to the cubic displacement x^3 . The equation has the form:

$$m\ddot{x} + c\dot{x} + kx + \alpha x^3 = A \cos(\omega t) \quad (1)$$

where t is time in (s), ω is the forcing frequency (rad/s), A is the forcing amplitude (N), α is the nonlinear stiffness coefficient (N/m³) and the k and c terms correspond to linear stiffness (N/m) and damping coefficient (Ns/m),

respectively. For convenience, a mass of $m = 1$ kg is assumed. If $\alpha = 0$ N/m, equation (1) becomes a linear system with constant stiffness, while $\alpha > 0$ results in a hardening spring and $\alpha < 0$ results in a softening spring.

To facilitate the calculation of periodic solutions using the numerical continuation technique, equation (1) is rewritten as the following fourth-order system:

$$\dot{x}_1 = x_2 \quad (2)$$

$$\dot{x}_2 = -kx_1 - cx_2 - \alpha x_1^3 + Ax_4 \quad (3)$$

$$\dot{x}_3 = x_3 + \omega x_4 - x_3(x_3^2 + x_4^2) \quad (4)$$

$$\dot{x}_4 = -\omega x_3 + x_4 - x_4(x_3^2 + x_4^2) \quad (5)$$

where equations (2) and (3) describe the first and second derivative of the state $x = x_1$, and equations (4) and (5) are the nonlinear oscillator used to generate the harmonic forcing term. It can be shown that $x_3 = \sin(\omega t)$ and $x_4 = \cos(\omega t)$. Using this relationship, the forcing term $A \cos(\omega t)$ becomes Ax_4 , as shown on the right-hand side of equation (3).

In order to calculate the frequency response, the forcing frequency ω is chosen as the continuation parameter. The four equations of motions are then solved for a chosen range of ω using the continuation algorithm, which generates a one-cycle periodic solution at each value of ω for all four states. As an example, two solutions to equation of (6) for the state x are shown in Figure 1.

$$\ddot{x} + 0.2\dot{x} + x + 0.05x^3 = 2.5 \cos(\omega t) \quad (6)$$

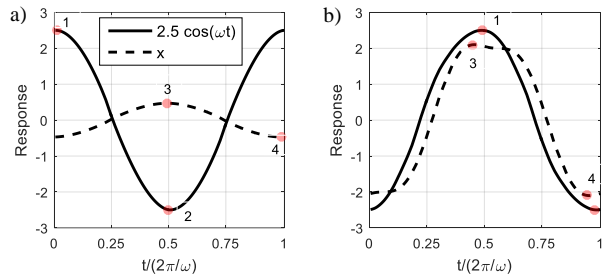


Fig 1 Periodic solutions to equation (6) of the state x at $\omega = 2.509$ rad/s (a) and $\omega = 0.298$ rad/s (b).

From Figure 1, the amplitude and phase of the oscillation are calculated using the following formula:

$$\text{amplitude} = \frac{Y_3 - Y_4}{2} \quad \text{or} \quad \text{amplitude in dB} = 20 \log_{10} \left(\frac{Y_3 - Y_4}{Y_1 - Y_2} \right) \quad (7)$$

$$\text{phase in degree} = (X_1 - X_3) \times 360 \quad (8)$$

where X_i and Y_i refer to the x and y-coordinates of point i in Figure 1.

Unlike in a linear system, the nonlinear forced response can contain multiple harmonics such as the case shown in Figure 1b. When this happens, the horizontal distance between points 1 and 3 no longer corresponds to the mathematical definition of phase in a linear forced system. Therefore, the phase diagram on the frequency response plot should see a small jump when the effect of additional harmonics becomes prominent. However, this way of determining the phase is deemed satisfactory as solutions that are not simple harmonic can be easily identified, which matches the main goal of determining regions where the nonlinear response differs from its linearized counterpart; the latter only produces simple harmonic sinusoidal outputs.

The frequency response of equation (6) is shown in Figure 2. The most notable difference from its linearized counterpart is the leaning of the solution curve, which is caused by the existence of the nonlinear term $\alpha = 0.05$. As a result, there are multiple possible responses for a single forcing frequency near resonance, which can be stable (solid line) or unstable (dashed line). To verify this phenomenon, the system is simulated with a slowly varying forcing frequency using a chirp signal. Data from the simulation is superimposed on the figure as a grey line and shows that the response will always follow the stable solutions. This indicates a dependency on the initial condition, which is a feature of nonlinear systems.

It is also noted that there are some additional small resonances at low frequencies known as subharmonic resonance. Its presence is also reflected in the phase jumps at the corresponding frequencies due to the additional harmonics introduced – one such case has been shown in Figure 1b. These harmonics can exist in a nonlinear system but are usually omitted in analytical solutions such as in [11] due to complexity. However, they can be easily detected using a numerical solver like AUTO. Due to their existence, a time history simulation picks up the ‘false peaks’ shown in Figure 3, which led to the apparent discrepancies between numerical and simulated results shown in Figure 2. In practical terms, this discrepancy is useful in detecting regions where the response is not simply harmonic when examining the simulated frequency response.

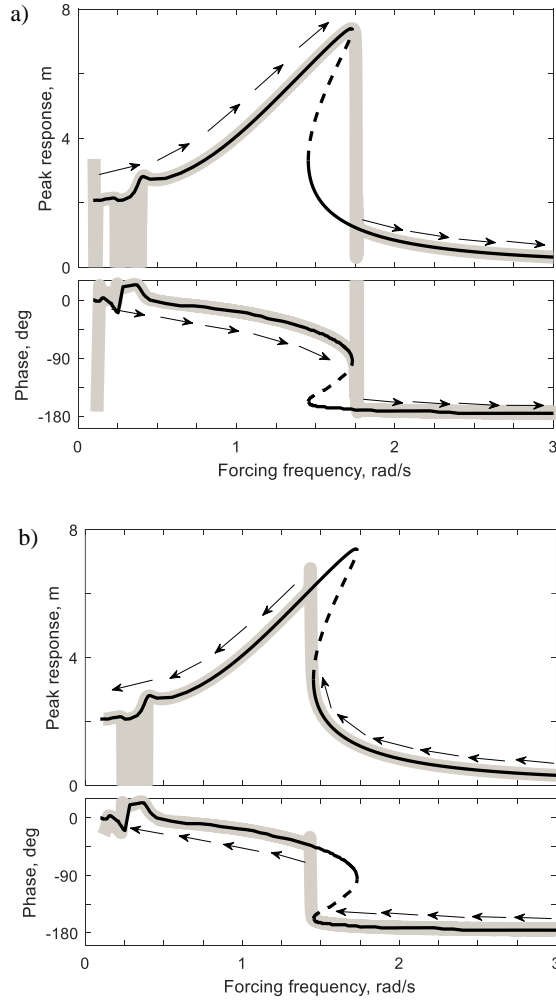


Fig 2 Frequency responses of equation (6) with time-stepping simulated frequency sweeps superimposed.

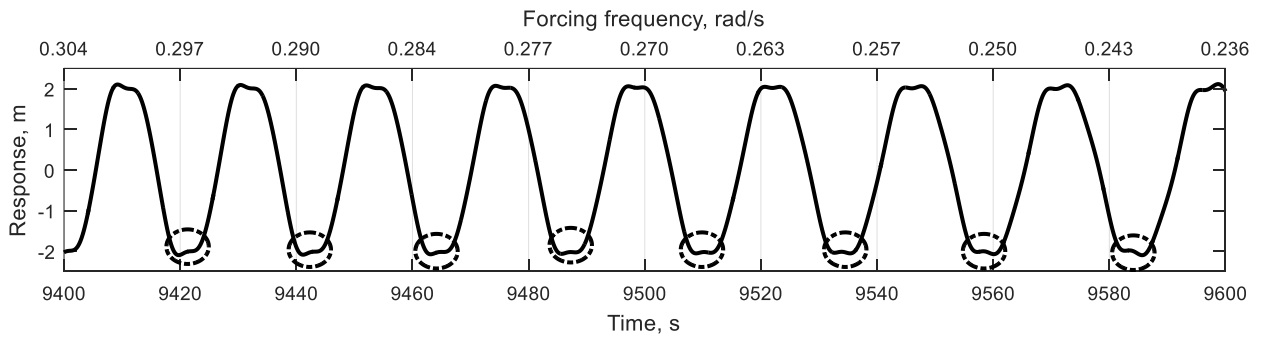


Fig 3 Time histories of the reducing frequency sweep as shown in Figure 2b. The ‘false peaks’ picked up by the code are circled.

Another notable feature in a nonlinear forced response is the dependency on the forcing amplitude. Figure 4 shows that increasing the forcing amplitude not only leads to larger responses but also makes the leaning of the resonance more prominent, which widens the region of multiple solutions. It is possible to identify the border of this region in the frequency-amplitude space using a technique called two-parameter continuation, which tracks the movement of the fold bifurcations (the point at which the solution folds back and creates a region of multiple solutions) as the forcing frequency and forcing amplitude change. The locus of the fold bifurcations is shown as a thin line in Figure 4, and its projection onto the ω - A plane is shown in Figure 5. It can be seen that if the forcing amplitude is small enough, the fold bifurcations disappear and only one stable solution exists for each forcing frequency, similar to what is seen in linear systems. Two-parameter continuation is a powerful technique that can be used to determine a nonlinear region's sensitivity to a system parameter.

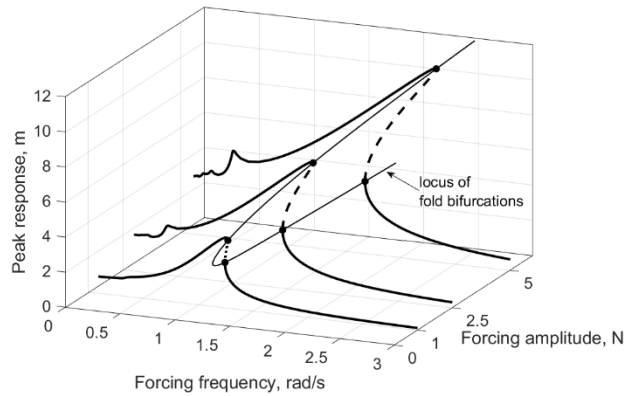


Fig 4 Frequency responses of equation (6) but for three different forcing amplitudes.

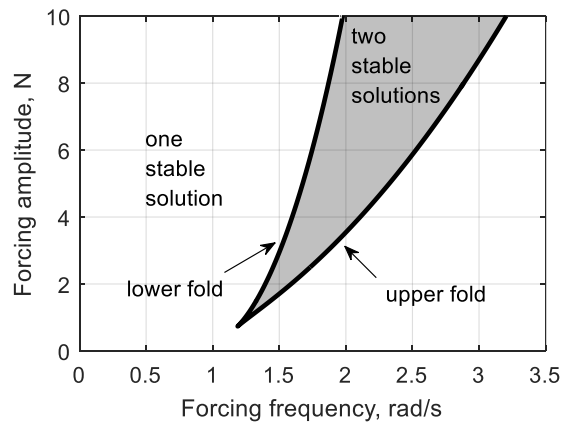







Fig 5 Two-parameter continuation of the fold bifurcation in the ω - A plane.

This section has illustrated the types of behavior that a nonlinear periodically forced system can produce as well as the tools used to study them. The validity of the techniques used on the continuation software AUTO to characterize a simple nonlinear forced system has also been demonstrated. In the following sections, the same technique is used to generate the forced response of an aircraft model to assess its frequency response. The list of symbols used in the nonlinear frequency response is shown in Table 1.

Table 1. Notation as used in the nonlinear frequency responses figures and bifurcation diagrams.

	Stable solution
	Unstable solution
	Torus bifurcation (the periodically forced response loses stability)
	Fold bifurcation
	Period-doubling bifurcation (the forced response repeats itself after twice the forcing cycle)

III. Description of the Aircraft Model

The methodology presented in this paper is applied to the NASA Generic Transport Model (GTM). The GTM is a nonlinear simulation of a 5.5% scale, remotely piloted, generic twin-under-wing engine civil transport aircraft, which was developed to study airliner upsets and loss-of-control. For this paper, two versions of the GTM are used:

1) Section VI uses the DesignSim implementation, which is a Matlab/Simulink nonlinear simulation of the 8th-order aircraft with avionics dynamics [24]. Its aerodynamic data is stored in lookup tables and are based on wind-tunnel tests for angles-of-attack between -5° and 85° and sideslip angles below 45° . For this paper, we utilized spline interpolation of the aerodynamic data to ensure smoothness for bifurcation analysis and ignored the influence of avionics – the same approach presented in [9, 10]. The DesignSim was chosen to show that the method can be applied to an industrial-standard aircraft model, as well as to demonstrate the complex dynamics encountered in such an application. This version is referred to as the ‘full GTM’.

2) A polynomial representation of the DesignSim is used in sections IV and V [8] where only longitudinal motions are considered, allowing us to reduce the model to 4th-order. Combined with the use of polynomials instead of lookup

tables, this version offers significant reducing in computation time. In addition, the polynomial model is also symmetric about the body x-z plane, unlike the real GTM, which simplifies the study and making it ideal to demonstrate our method. Table 2 lists the two operating points to be studied, which represent medium and high angles of attack, and Figure 6 shows the positions of their roots in the complex plane. The aircraft is trimmed in straight-and-level horizontal flight in both cases by adjusting the elevator deflection and throttle. This is appropriate as linear gain-scheduled controllers are typically designed around the trim points. This version is referred to as the ‘polynomial GTM’.

Table 2. Operating points to be studied

Operating point	$\alpha = \theta$ (deg)	V (m/s)	q (deg/s)	δ_e (deg)	Throttle	Description
1	9	29.6	0	0.68	12.7%	Phugoid mode is marginally damped
2	18	25	0	-7.2	59%	Short period mode is unstable

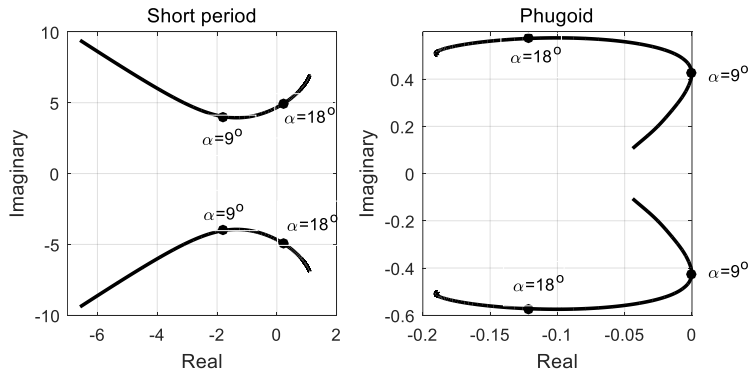


Fig 6 Longitudinal root loci of the polynomial GTM for elevator deflections between -30° and 6° .

IV. Longitudinal dynamics at medium angle-of-attack ($\alpha = 9^\circ$)

In this section, the frequency response at 9° angle-of-attack is used to demonstrate how continuation analysis can reveal the effect of the controller gain on the aircraft’s dynamics in the frequency domain. The polynomial GTM is trimmed for straight-and-level flight at 29.6 m/s (see Table 2). First, considering the open-loop dynamics, the pitch-

angle-to-elevator Bode plots are shown in Figure 7a for the linear model and Figure 7b for the nonlinear model. For clarity, bifurcation symbols are not shown in Figure 7b. However, they are shown in the magnified view given in Figure 9a. Apart from the two peaks at the phugoid and short-period frequencies (0.07 Hz and 0.60 Hz), the nonlinear model contains additional peaks at low frequencies (between 0.017 and 0.035 Hz), known as subharmonic resonance, as well as a peak at 0.14 Hz (to the right side of the phugoid resonance) due to a pair of period-doubling bifurcations; all of which are not captured in the linear model. The peak at 0.14 Hz can be referred to as superharmonic resonance. Additionally, the resonance curves in the nonlinear response lean to the right, indicating that the aircraft resembles a hardening system (i.e. the restoring force increases with higher oscillation amplitude, which is expected for a dynamically stable airliner). Unstable solutions are seen in the nonlinear response, which cause the aircraft to diverge if it is forced at one of those frequencies.

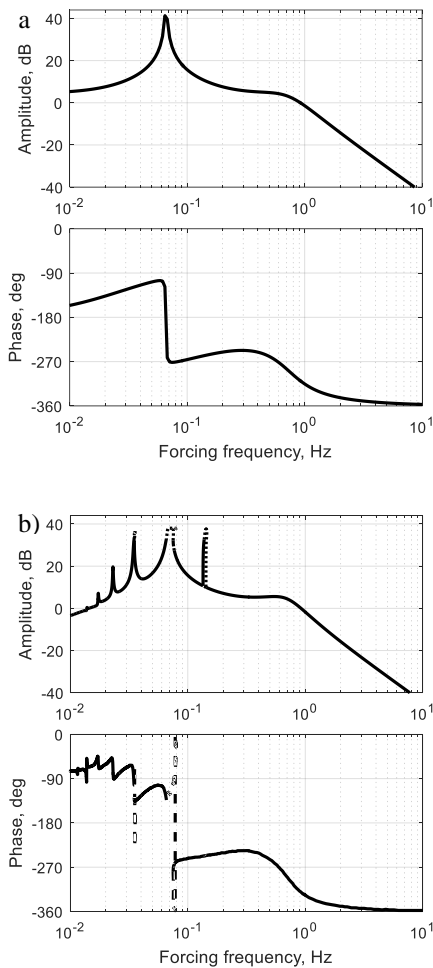


Fig 7 Linear (a) and nonlinear (b) open-loop pitch-angle-to-elevator Bode plots at $\alpha = 9^\circ$.

As the nonlinear dynamics and instability observed in this region are caused by the phugoid mode being marginally damped (see Figure 6), a common method to improve stability is to use pitch angle feedback. For this study, a simple proportional stability augmentation controller as shown in Figure 8 is used, and the elevator demand signal is given a harmonic input in the form of $\cos(\omega t)$. The effect of increasing the proportional gain from zero on the elevator-demand-to-pitch-angle frequency response will be studied, which we will refer to as the elevator-to-pitch-angle frequency response (with the word ‘demand’ omitted).

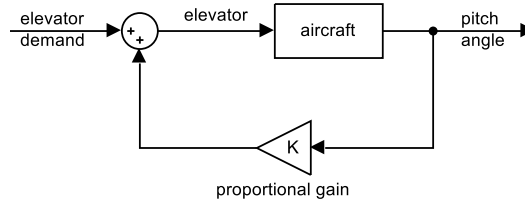


Fig 8 Proportional stability augmentation controller.

Figure 9 shows how the nonlinear frequency response is modified due to the controller gain increasing from 0 to 0.08, and Table 3 summarizes the notable changes. The rest of this section will explain how numerical continuation is used to identify the features listed in Table 3.

Table 3. Summary of the frequency responses in Figure 9.

Gain	Figure	Description
0	9a	Open-loop frequency response (note the change of y-axis unit from dB to deg).
0.00046	9b	The unstable subharmonic resonance detaches from the main branch and forms an isola.
0.00820	9c	The unstable superharmonic resonance detaches from the main branch and forms an isola.
0.014	9d	The stable superharmonic (period-2) resonance disappears.
0.024	9e	The unstable phugoid resonance detaches from the main branch and form an isola.
0.080	9f	Most of the subharmonic resonance is suppressed.
0.113	not shown	The isola formed by the superharmonic (period-2) resonance disappears.
0.129	not shown	The isola formed by the subharmonic resonance disappears.
0.148	not shown	The isola formed by the phugoid resonance disappears.

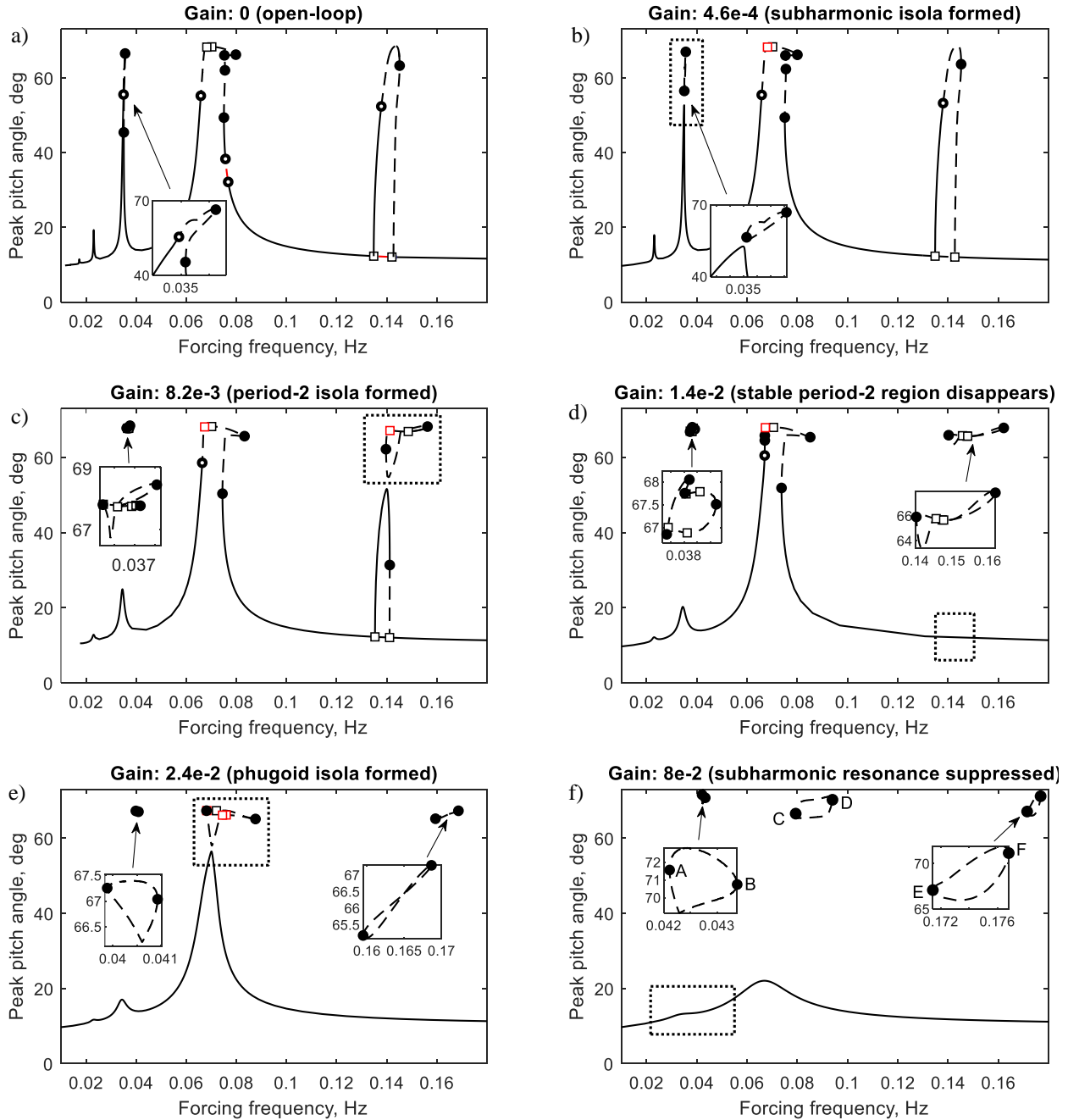


Fig 9 Frequency responses at different controller gains. The dotted rectangles are used to highlight the notable features; solid rectangles are magnified views.

A. Detecting the formation of isolas

The inset panels in figures 9a and 9b show the process of the unstable solutions in the subharmonic resonance detaching from the main branch as the controller gain increases from 0 to 0.00046. This process is shown in more

detail in Figure 10 with an intermediate step at gain 0.00040. The isola is formed when the torus bifurcation and the lower fold bifurcation collide, which ‘connects’ the stable solutions while ‘cutting off’ the unstable solutions from the main branch. Detecting isolas using numerical continuation is difficult as the method can only map out the solutions connected to the initial solution supplied by the user. However, this can be overcome by tracing the movement of the bifurcation points (fold and torus bifurcations in this case) using two-parameter continuation, shown as the blue and grey lines in Figure 10. When an isola formation is suspected, such as when the torus and fold bifurcation collide, one of the fold bifurcation points can be then used as the initial solution and the isola can then be traced.

To verify that the divergent motion due to unstable solutions no longer exists, the aircraft is forced at the frequency 0.03503 Hz using the three different controller gains shown in Figure 10. Their time histories (Figure 11) show that in the first two cases (gains 0 and 0.00040), the responses still diverge to infinity, leading to the simulation failing, while in the third case (gain 0.00046), the response is stable, confirming that the unstable solution has been removed from the main branch. Although all solutions in the isola are unstable in this case, which removes the possibility of two possible responses for the same forcing frequency (one in the main branch and one in the isola with much higher amplitude), the presence of the unstable isola can still influence dynamic response in this region, e.g. in the case of a large pitch disturbance.

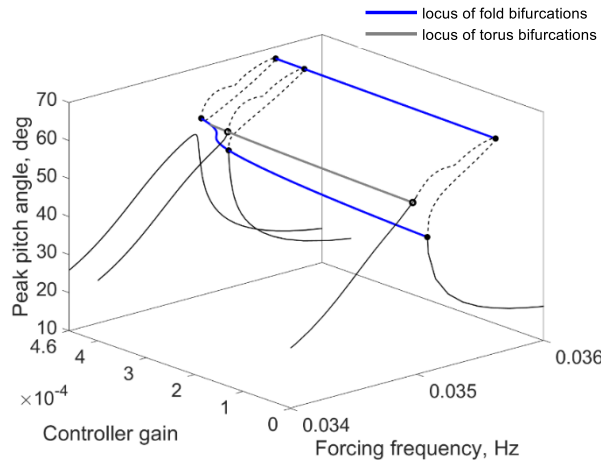
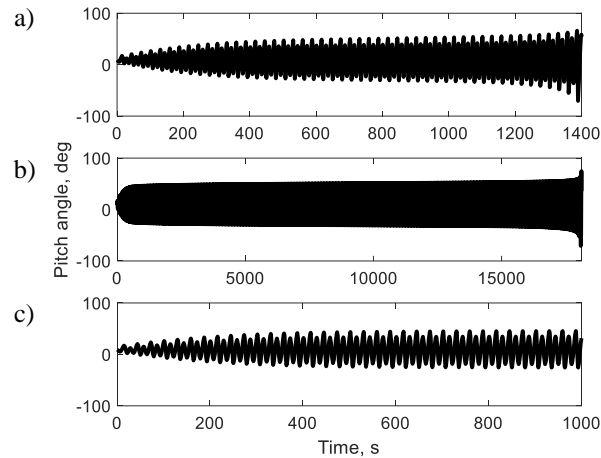


Fig 10 Formation of the isola in the subharmonic resonance region.



**Fig 11 Simulated response of the aircraft forced at 0.03503 Hz for three controller gains:
0 (a), 4.0×10^{-4} (b), and 4.6×10^{-4} (c).**

Using the same technique, the isolas formed in the superharmonic and phugoid resonances can also be traced. The point at which they detach from the main branch are shown in figures 9c and 9e.

B. Eliminating the superharmonic (period-2) resonance

In the period-2 superharmonic region (see Figure 9a), the aircraft's response repeats itself after two instead of one forcing cycle – a highly nonlinear behavior that is not captured in the linear model. Figure 12 shows the simulation results when the aircraft is forced at 0.137 Hz and 0.138 Hz, corresponding to the stable and unstable solutions in the period-2 region, respectively. In both cases, period-2 motions are observed, and the oscillation amplitude is very large compared to the linear model's prediction at these frequencies. When the forcing frequency lies within the unstable region such as in the second case (0.138 Hz), the aircraft diverges. This large amplitude period-2 motion is undesirable.

Using our proportional pitch-angle-feedback controller, we cannot rely on linear design techniques to determine the controller's effectiveness in eliminating the period-2 region as this motion is not captured by the linear model. Instead, the two-parameter continuation technique can be used to determine the controller's effectiveness by tracking the movement of the period-doubling bifurcation in the frequency-proportional gain space – thereby providing information on how the period-2 region is modified as the controller gain increases. The result in Figure 13 shows that as the controller gain increases, the two period-doubling bifurcations approach each other, reducing the size of the period-2 region, and finally merge when the controller gain reaches 0.01379, meaning that this is the minimum gain required to eliminate the period-2 motion. To verify this, the aircraft is forced again at 0.138 Hz but with the gain set

at 0.0140, shown in Figure 14. Comparing to Figure 12b, the oscillation is now stable and has the same period as the forcing term, confirming that the period-doubling bifurcations no longer exist in the main solution branch.

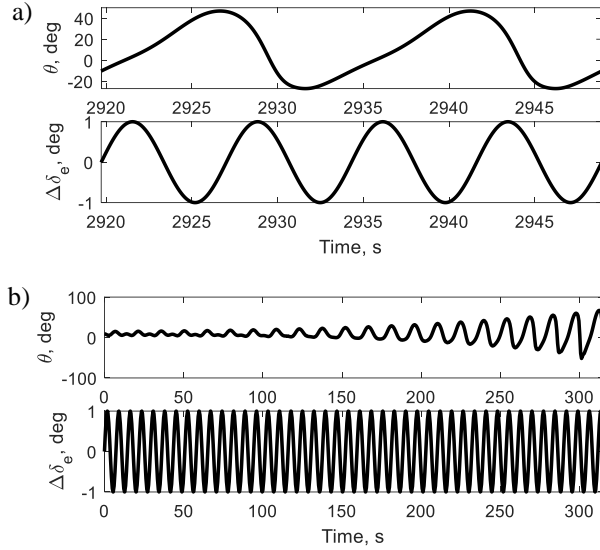


Fig 12 Open-loop period-2 response at 0.137 Hz (a) and 0.138 Hz (b).

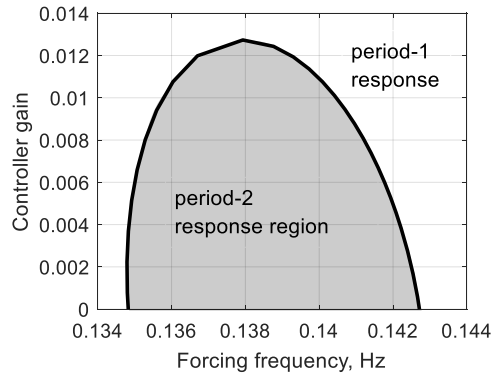


Fig 13 Locus of the period-doubling bifurcations.

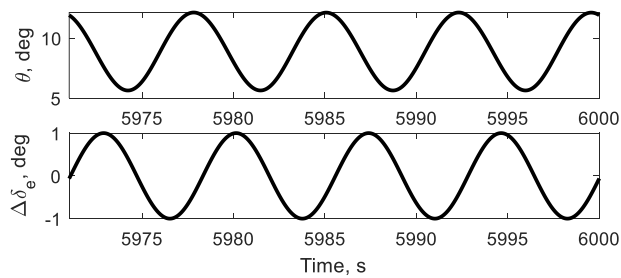


Fig 14 Closed-loop response at 0.138 Hz with gain 0.014.

C. Eliminating the subharmonic resonance

Figure 9e shows that at gain 0.024, all unstable and divergent solutions have been removed from the main branch, so the forced response is stable at all frequencies. However, the subharmonic resonance is still prominent at frequencies below the phugoid resonance, so a higher controller gain is needed to remove them. Since there is no longer any bifurcation on the main branch, two-parameter continuation cannot be used. Instead, one-parameter continuation of the controller gain is utilized. Referring back to Figure 7a, it is known from the standard elevator-to-pitch-angle transfer function of the linear model that below the phugoid frequency (0.065 Hz), the response amplitude is proportional to the forcing frequency (i.e. higher forcing frequency leads to larger response, up to 0.065 Hz). This is not the case in the nonlinear model in the presence of the subharmonic resonance peaks. It is desirable to know the controller gain required to remove these subharmonic resonances, therefore making the full aircraft behave more like its linear counterpart. To do this, one-parameter continuation of the controller gain is done at two frequencies: 0.0350 Hz (near the peak of the subharmonic resonance in Figure 9a) and a nearby point at higher frequency, chosen as 0.0385 Hz in this case. The result in Figure 15 shows that as the controller gain increases from 0, the response amplitude at the lower frequency (0.0350 Hz) rapidly decreases and eventually becomes lower than the response at the higher frequency (0.0385 Hz) for controller gain beyond 0.07. This shows that in order to remove the subharmonic resonance, the controller gain cannot be less than 0.07. As shown in Figure 9f, at gain 0.08, most of the subharmonic resonance has been removed.

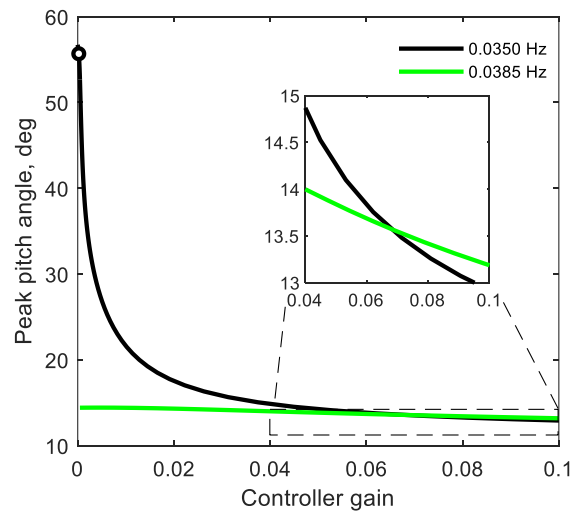


Fig 15 Continuation of the controller gain at the subharmonic region for two different frequencies.

D. Eliminating the unstable isolas

Figure 9f indicates that at gain 0.08, the nonlinear frequency response is stable across the entire frequency range considered and resembles a linearized response. However, the three unstable isolas that emerged from the subharmonic, phugoid, and superharmonic resonances still exist and can influence the aircraft's dynamics, such as in the case of a large disturbance. The edges of these isolas are three pairs of fold bifurcations labelled A to F. Again, by using two-parameter continuation to track the movement of these fold bifurcations, the gain required to remove each isola can be determined. Figure 16 shows the two-parameter continuation of the points A to F as the controller gain changes. Despite their complex trajectory, it can be seen that each pair of fold bifurcation will merge when the controller is high enough, indicating the disappearance of the isola. The gains required to remove each isola are listed as the last three items the of Table 3. For a gain above 0.148, the final isola that emerges from the phugoid resonance ceases to exist.

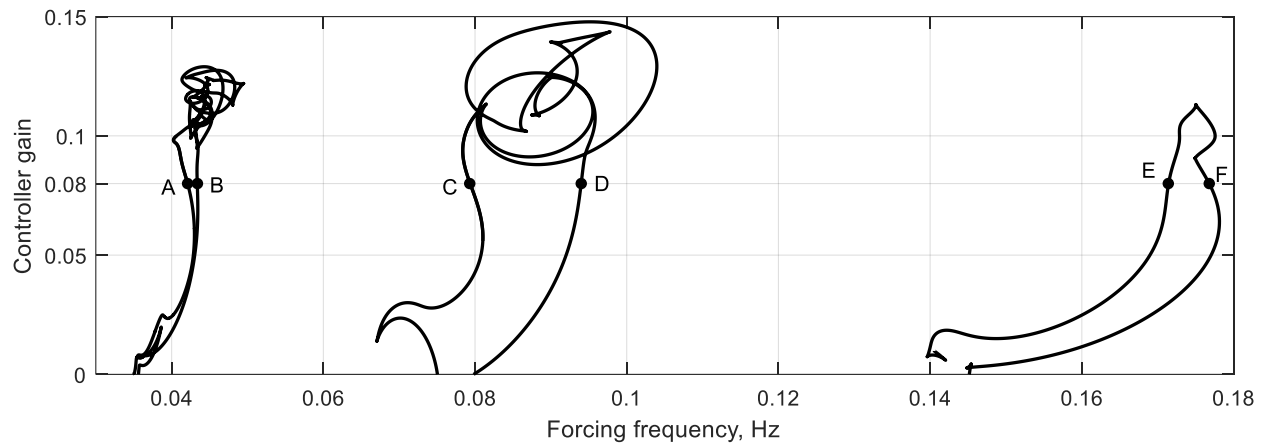


Fig 16 Two-parameter continuation of all fold bifurcations shown in Figure 9f.

In summary, this section has so far shown the advantages of using nonlinear analysis in identifying the undesirable dynamics in the frequency domain that are not captured by the linear model. Using both one and two-parameter continuation of the controller gain, we can assess the controller's effectiveness in removing those undesirable attractors.

V. Longitudinal dynamics at higher angle-of-attack ($\alpha = 18^\circ$)

Now we consider the polynomial GTM trimmed for straight-and-level flight 18° angle-of-attack (see Table 2). The short-period mode is unstable at this operating point, and the unforced aircraft enters a limit cycle – a self-sustaining bounded oscillation – without any external input. Forcing the open-loop aircraft at this angle-of-attack will result in motions that appear to be quasi-periodic as shown in Figure 17. The linear model cannot capture this behavior but can only indicate that the aircraft is unstable. Therefore, the linear aircraft diverges to infinity as soon as it is perturbed from the trim condition, whether forced or unforced. Due to these differences, the open-loop frequency response is not considered in this section.

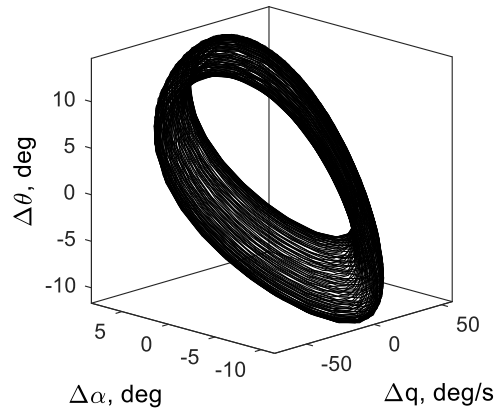


Fig 17 Phase plot of the open-loop nonlinear aircraft responding to an elevator forcing at 1 Hz.

To stabilize the short-period mode, a pitch-rate-feedback controller with proportional gain 0.05 is used (similar to the scheme in Figure 8 but using pitch rate for the feedback signal). Figure 18 compares the linear and nonlinear closed-loop unforced responses when subjected to an elevator perturbation of 0.1° and duration 0.1s. Whilst the short-period responses are similar, it can be seen that the low-frequency content from the phugoid mode is much less damped in the nonlinear model.

The reduced damping of the phugoid mode in the nonlinear response is more clearly reflected in the frequency domain. Figure 19 compares the linear and nonlinear closed-loop frequency responses, where large discrepancies are seen at low frequencies. In particular, a large difference in gain and phase is observed around the phugoid frequency, approximately near 10^{-1} Hz. As the forcing frequency is reduced further, the gain again becomes similar while the

phase difference increases to as high as 180° . This means that at low frequencies, the nonlinear pitch angle response is completely out of phase with the linear response and hence with the pilot input. To verify this, the linear and nonlinear models are simulated with a harmonic elevator input of magnitude 1° and frequency 0.07358 Hz (Figure 20). This frequency was chosen as it is near the peak of the phugoid resonance, where the largest discrepancies in both gain and phase are observed between the linear and nonlinear models. It can be seen that although the controller has stabilized the aircraft, the responses are completely out of phase and have different magnitudes. Although this reduction in handling quality is not captured by the linear model, the use of continuation methods can provide insights on the issue, specifically to inform the control designers that further investigation is required.

This section has presented an example in which the linear model cannot adequately capture the aircraft dynamics. The use of closed-loop forced response and two-parameter continuation have been shown to be useful in informing the control designer of the lack of robustness of the controller in both the frequency and time domains.

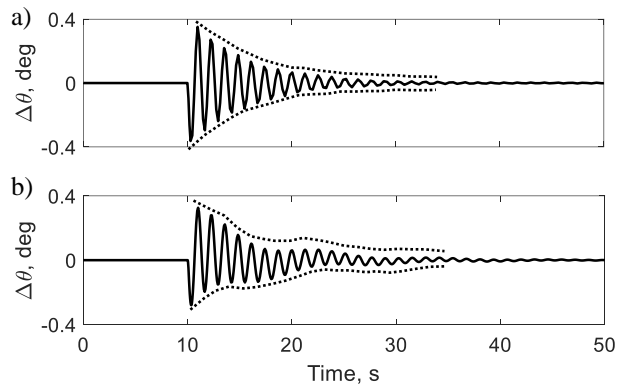


Fig 18 Linear (a) and nonlinear (b) closed-loop aircraft responding to an elevator perturbation.

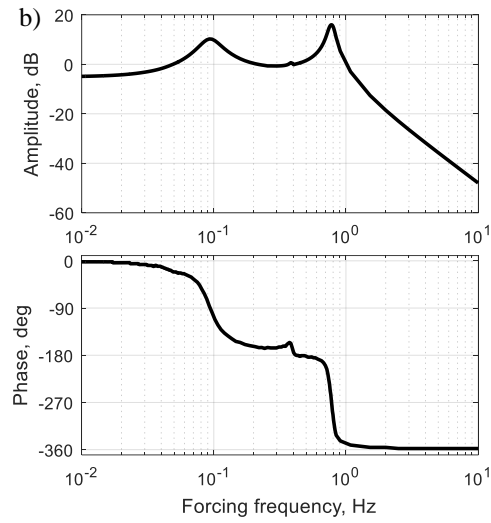
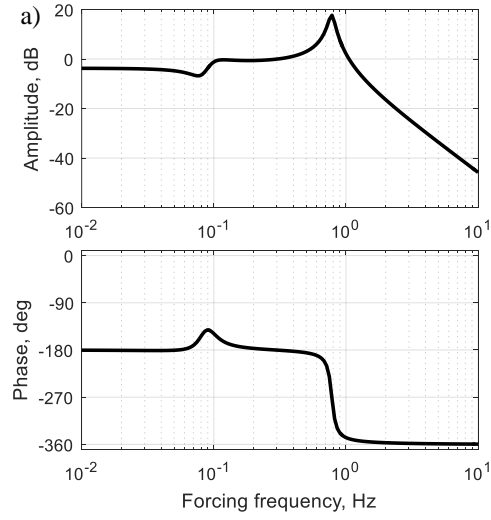


Fig 19 Linear (a) and nonlinear (b) closed-loop pitch-angle-to-elevator Bode plots.

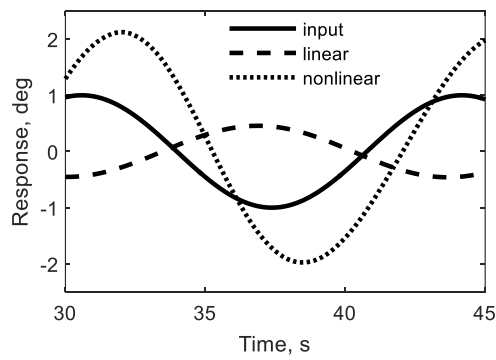


Fig 20 Linear and nonlinear closed-loop response at 0.07358 Hz.

VI. Lateral-directional behavior at medium angle-of-attack ($\alpha = 9^\circ$)

To further highlight the complex dynamics in the frequency domain purely due to aerodynamic nonlinearities, this section presents a brief investigation on aileron and rudder forcing of the 8th-order open-loop full GTM. All analysis was done with the aircraft trimmed at 8.7° angle-of-attack, where the phugoid instability is observed as discussed previously. Because the full GTM is asymmetric, any perturbation to one of its control surfaces will induce both longitudinal and lateral-directional motions.

A. Aileron forcing

The open-loop aileron-to-bank-angle frequency responses of the linearized and nonlinear GTM are shown in Figure 21. The inset in the nonlinear frequency response highlights a region with three stable solutions at just below 0.062 Hz. Their existence is verified in time simulation (Figure 22). As a result, the same forcing frequency will lead to three very different responses with a peak pitch angle of around 9° , 30° , and 50° . The aircraft's initial condition will determine which of these three stable solutions the aircraft converges to.

To further investigate this phenomenon, we ran a large number of simulations at 0.0617 Hz with different initial yaw and bank angles while keeping the remaining six initial states at their trim values. Figure 23 shows the result of those simulations with the initial bank and side slip angles on the x and y axis. The color of each point indicates peak pitch angle in the final oscillation cycle after a 1000s simulation, which would converge to one of the three stable solutions of θ (9° , 30° , and 50° ; the first one corresponds to normal flight). From Figure 23, the following observations can be made:

- The normal flight response (9° – blue) dominates the central-right region, which indicates the asymmetric nature of the GTM.
- The highest amplitude response (50° – yellow) is the least likely to occur. However, it can scatter almost randomly in a green-dominant region. One such example is shown in the magnified view, in which for the same sideslip angle of 0° , the three bank angles of -13° , -12° , and -11° converge to three different solutions. This means that changing the initial condition by just one degree can result in a vastly different response, which highlights the nonlinear nature of the GTM. Similar behavior can also be observed in other sections of Figure 23.

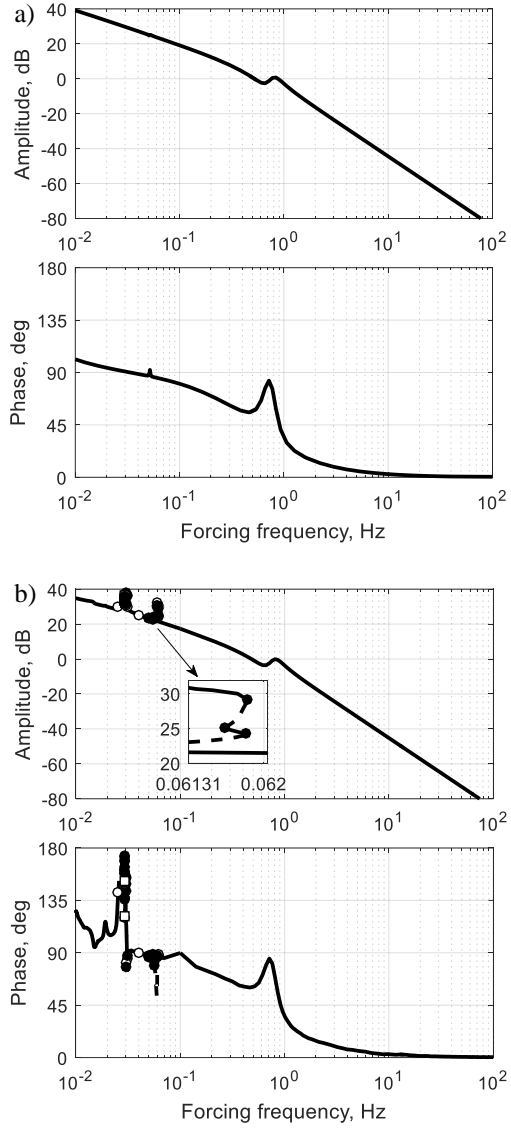


Fig 21 Linear (a) and nonlinear (b) aileron-to-bank-angle frequency response.

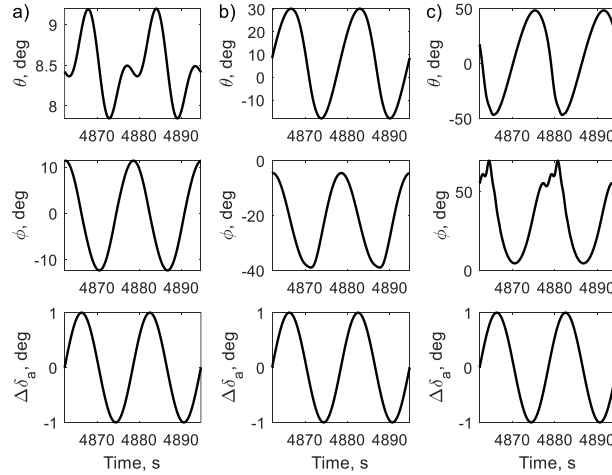


Fig 22 Three different possible responses to aileron forcing at 0.0617 Hz.

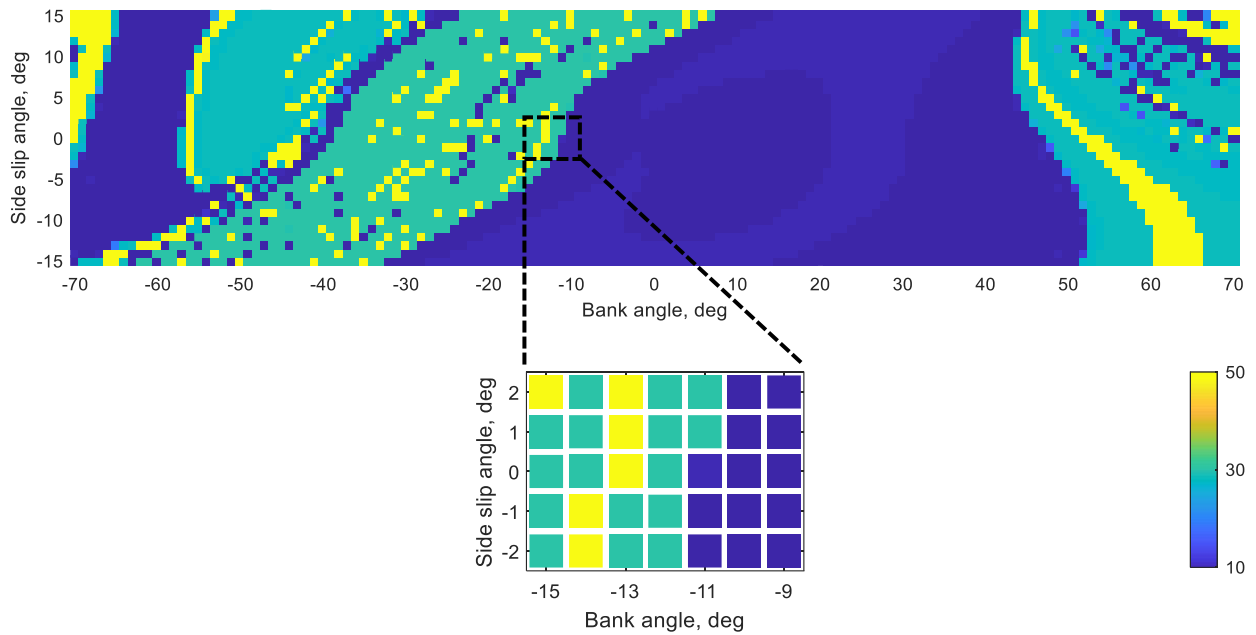


Fig 23 Basin of attraction of the full open-loop GTM due to aileron forcing at 0.0617 Hz.

B. Rudder forcing

The linear and nonlinear open-loop rudder-to-yaw-rate frequency responses are shown in Figure 24. A pair of torus bifurcation between 0.63 and 0.78 Hz (near the middle of Figure 24b) results in a region of stable quasi-periodic response (see Figure 25 for the simulation). Additionally, the inset in the nonlinear frequency response indicates a pair of period-doubling bifurcation, which gives rise to a very complex period-7 motion shown in Figure 26.

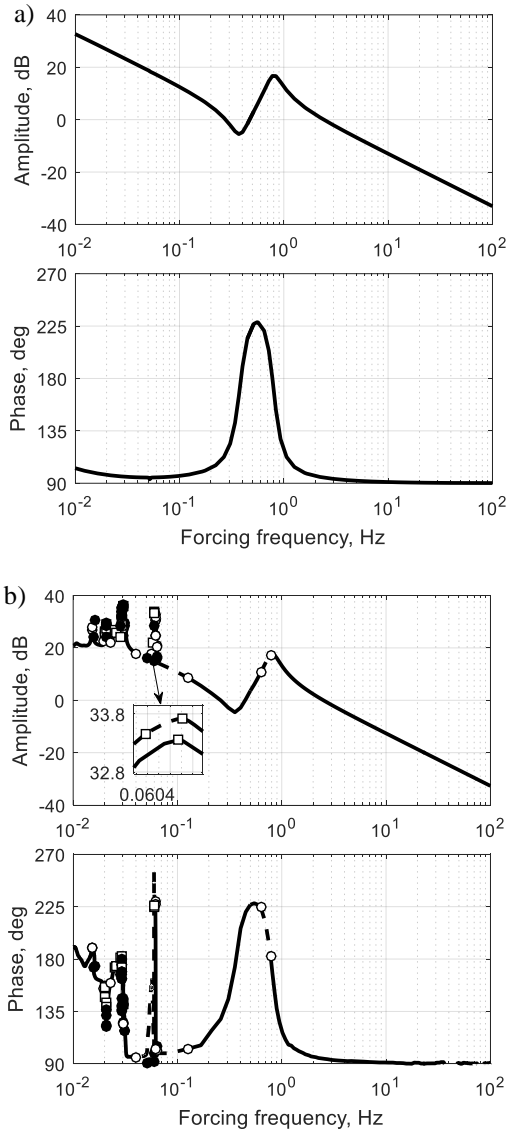


Fig 24 Linear (a) and nonlinear (b) rudder-to-yaw-rate frequency responses.

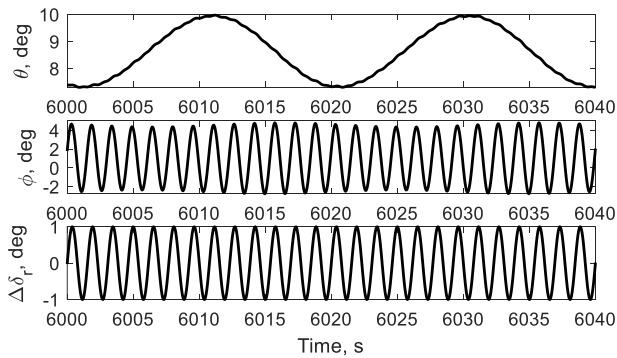


Fig 25 Quasi-periodic motion at 0.65 Hz rudder forcing.

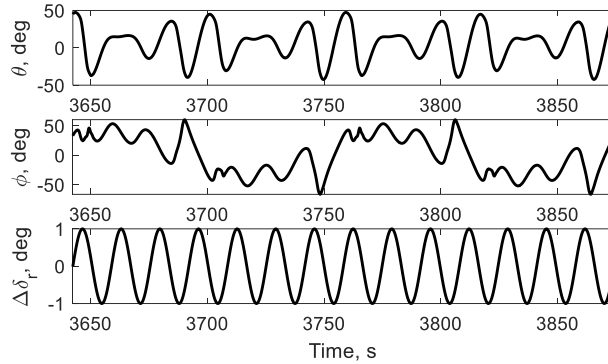


Fig 26 Period-7 motion at 0.0604 Hz rudder forcing.

Although the aileron and rudder are lateral-directional control surfaces, it has been shown that exciting them near the phugoid frequency can lead to high-amplitude oscillations in both the longitudinal and lateral-directional planes. This suggests some forms of modal interactions between the conventional flight dynamics modes due to the asymmetry of the aircraft model. The rich dynamics that are revealed also illustrates the nonlinear nature of the GTM. The same approach can be applied to more complex systems where nonlinear modal interaction is significant, such as in a highly flexible aircraft in which the structural dynamics is modelled.

VII. Conclusions

This paper has presented methods of generating the nonlinear frequency responses of an aircraft model using numerical continuation. It has been shown that the technique gives a clear indicator of where the behavior of the linearized model may differ significantly from that of the full model. The technique is applicable to both open and closed-loop analysis. Classical controller design methods rely on linearized models, which do not capture all the dynamics, especially at high angles of attack or during rapid maneuvering where nonlinearity becomes significant. On the other hand, the use of both one and two-parameter continuations in controller gain proved useful in determining the controller's effectiveness in eliminating the undesirable attractors that either degrade the aircraft's handling qualities or lead to dynamics that are completely uncaptured by the linear model. Therefore, the information gained from the nonlinear frequency response will help determine whether the controller performs as predicted when implemented on the nonlinear model. The adoption of a periodically forced bifurcation and continuation method

approach also allows the contributions of any time-dependent phenomena in the model to be captured, which conventional equilibria solutions would not do. Frequency domain studies of nonlinear flight mechanics models are currently seldom considered in both industry and academia. However, we have shown that the technique provides useful insights, especially given the drive to move toward flight dynamics models that are extended to represent unsteady aerodynamic phenomena.

The nonlinear dynamics in the frequency domain shown in a simple longitudinal aircraft model example are prominent at higher angles of attack as the aircraft enters the stall region, which has the potential for undesirable responses such as upsets and loss-of-control. Specifically, the frequency responses of the aircraft with and without a stability-augmentation controller have been assessed. Large discrepancies in gain and phase between the linear and nonlinear frequency responses are seen at low frequencies, where the influence of the phugoid mode is significant. In particular, the extra resonances below the phugoid frequency and the large-amplitude period-2 motion are undetected by the linear model. A controller operating in the period-2 region may perform inadequately if the gain is not sufficiently large or go completely out of phase and cause much larger responses than predicted if it is operated in the subharmonic resonance region. It should be noted that the polynomial model used in this study was defined to represent the marginal phugoid stability of the full GTM at medium angle of attack, so it is expected that nonlinear behaviors are only observed at low frequencies, and that the model is not particularly representative of the other flight dynamics modes. However, the techniques proposed can be employed on more complex industrial-standard models as seen in the brief analysis of the full GTM, which shows the potential of the method on highly nonlinear applications where modal interactions between different elements of the system are significant.

Funding source

The authors gratefully acknowledge the financial support from the University of Bristol's Alumni Grant, which provides partial funding for the first author's PhD.

References

1. Carroll, J. V., and Mehra, R. K. "Bifurcation Analysis of Nonlinear Aircraft Dynamics," *Journal of Guidance, Control, and Dynamics*, Vol. 5, No. 5, 1982, pp. 529-536.
doi: 10.2514/3.56198

2. Goman, M. G., Zagainov, G. I., and Khramtsovsky, A. V. "Application of Bifurcation Methods to Nonlinear Flight Dynamics Problems," *Progress in Aerospace Sciences*, Vol. 33, No. 9-10, 1997, pp. 539-586.
doi: 10.1016/S0376-0421(97)00001-8
3. Sinha, N. K. "Applications of Bifurcation Methods to F-18/HARV Open-loop Dynamics in Landing Configuration," *Defence Science Journal*, Vol. 52, No. 2, 2002, pp. 103-115.
4. Guicheteau, P. "Bifurcation theory: a tool for nonlinear flight dynamics," *Philosophical Transactions of the Royal Society of London. Series A: Mathematical, Physical and Engineering Sciences*, Vol. 356, No. 1745, 1998, pp. 2181-2201.
doi: 10.1098/rsta.1998.0269
5. Avanzini, G., and Matteis, G. d. "Bifurcation Analysis of a Highly Augmented Aircraft Model," *Journal of Guidance, Control, and Dynamics*, Vol. 20, No. 4, 1997, pp. 754-759.
doi: 10.2514/2.4108
6. Macmillen, F. B. J., and Thompson, J. M. T. "Bifurcation analysis in the flight dynamics design process? A view from the aircraft industry," *Philosophical Transactions of the Royal Society of London. Series A: Mathematical, Physical and Engineering Sciences*, Vol. 356, No. 1745, 1998, pp. 2321-2333.
doi: 10.1098/rsta.1998.0276
7. Richardson, T., Lowenberg, M., DiBernardo, M., and Charles, G. "Design of a Gain-Scheduled Flight Control System Using Bifurcation Analysis," *Journal of Guidance, Control, and Dynamics*, Vol. 29, No. 2, 2006, pp. 444-453.
doi: 10.2514/1.13902
8. Kwatny, H. G., Dongmo, J.-E. T., Chang, B.-C., Bajpai, G., Yasar, M., and Belcastro, C. "Nonlinear Analysis of Aircraft Loss of Control," *Journal of Guidance, Control, and Dynamics*, Vol. 36, No. 1, 2013, pp. 149-162.
doi: 10.2514/1.56948
9. Gill, S. J., Lowenberg, M. H., Neild, S. A., Krauskopf, B., Puyou, G., and Coetzee, E. "Upset Dynamics of an Airliner Model: A Nonlinear Bifurcation Analysis," *Journal of Aircraft*, Vol. 50, No. 6, 2013, pp. 1832-1842.
doi: 10.2514/1.C032221

10. Gill, S. J., Lowenberg, M. H., Neild, S. A., Crespo, L. G., Krauskopf, B., and Puyou, G. "Nonlinear Dynamics of Aircraft Controller Characteristics Outside the Standard Flight Envelope," *Journal of Guidance, Control, and Dynamics*, Vol. 38, No. 12, 2015, pp. 2301-2308.
doi: 10.2514/1.G000966
11. Holmes, P. J., and Rand, D. A. "The bifurcations of Duffing's equation: An application of catastrophe theory," *Journal of Sound and Vibration*, Vol. 44, No. 2, 1976, pp. 237-253.
doi: 10.1016/0022-460x(76)90771-9
12. Nayfeh, A. H., and Sanchez, N. E. "Bifurcations in a forced softening duffing oscillator," *International Journal of Non-Linear Mechanics*, Vol. 24, No. 6, 1989, pp. 483-497.
doi: 10.1016/0020-7462(89)90014-0
13. Bennett, J. A., and Eisley, J. G. "A multiple degree-of-freedom approach to nonlinear beam vibrations," *AIAA Journal*, Vol. 8, No. 4, 1970, pp. 734-739.
doi: 10.2514/3.5749
14. Xia, M., and Sun, Q. "Jump phenomena of rotational angle and temperature of NiTi wire in nonlinear torsional vibration," *International Journal of Solids and Structures*, Vol. 56-57, 2015, pp. 220-234.
doi: 10.1016/j.ijsolstr.2014.11.002
15. Benedettini, F., Rega, G., and Alaggio, R. "Non-linear oscillations of a four-degree-of-freedom model of a suspended cable under multiple internal resonance conditions," *Journal of Sound and Vibration*, Vol. 182, No. 5, 1995, pp. 775-798.
doi: 10.1006/jsvi.1995.0232
16. Rega, G., and Benedettini, F. "Planar non-linear oscillations of elastic cables under subharmonic resonance conditions," *Journal of Sound and Vibration*, Vol. 132, No. 3, 1989, pp. 367-381.
doi: 10.1016/0022-460x(89)90631-7
17. Jacobson, S., Britt, R., Freim, D., and Kelly, P. "Residual pitch oscillation (RPO) flight test and analysis on the B-2 bomber," *39th AIAA/ASME/ASCE/AHS/ASC Structures, Structural Dynamics, and Materials Conference and Exhibit*. AIAA, Paper 98-25095, Long Beach, CA, 1998.
18. Baghdadi, N. M., Lowenberg, M. H., and Isikveren, A. T. "Analysis of Flexible Aircraft Dynamics Using Bifurcation Methods," *Journal of Guidance, Control, and Dynamics*, Vol. 34, No. 3, 2011, pp. 795-809.

doi: 10.2514/1.51468

19. Mehra, R. K., and Prasanth, R. K. "Bifurcation and limit cycle analysis of nonlinear pilot induced oscillations," *23rd Atmospheric Flight Mechanics Conference*. AIAA, Paper A98-37220, Boston, MA, 1998.
20. Gránásy, P., Thomasson, P. G., Sørensen, C. B., and Mosekilde, E. "Non-linear flight dynamics at high angles-of-attack," *The Aeronautical Journal*, Vol. 102, No. 1016, 1998, pp. 337-344.
doi: 10.1017/S0001924000027585
21. Krauskopf, B., Osinga, H. M., and Galán-Vioque, J., *Numerical continuation methods for dynamical systems: path following and boundary value problems*, Springer, Dordrecht, 2007.
22. Coetzee, E., Krauskopf, B., and Lowenberg, M. "The dynamical systems toolbox: Integrating AUTO into Matlab," *16th US National Congress of Theoretical and Applied Mechanics*. Pennsylvania State University, Paper USNCTAM No. USNCTAM2010-827, State College, PA, 2010.
23. Doedel, E. "*AUTO-07P, Continuation and Bifurcation Software for Ordinary Differential Equations, Ver. 07P*", <http://www.macs.hw.ac.uk/~gabriel/auto07/auto.html> [retrieved 1 November 2019].
24. Anonymous. "*GTM_Polysim-Nonlinear GTM Aircraft Polynomial Simulation in MATLAB, Version 2.0*", <https://software.nasa.gov/software/LAR-17595-1> [retrieved 17 July 2020].